Intra-surface radiative transfer limits the geographic extent of snow penitents on horizontal snowfields

L. Maclagan CATHLES,* Dorian S. ABBOT, Douglas R. MacAYEAL

Department of Geophysical Sciences, University of Chicago, Chicago, IL, USA
E-mail: mcathles@umich.edu

ABSTRACT. Penitents are broad snow spikes and ridges that range in height between centimeters and meters. Two key features of penitents remain unexplained: (1) they generally form at low latitudes and (2) their ridges and troughs have an east–west orientation. Here we show that surface-to-surface exchange of shortwave radiation and the local geometry of the sun's daily arc across the sky are the key processes that, in the absence of other effects, determine the geographic extent of where surface roughness features can grow or dissipate on snowfields and ice surfaces. As an application of our analysis, we examine the question of the geographic extent of snow penitents on horizontal surfaces. The results show that surface-to-surface radiative transfer can explain why penitents do not form on horizontal surfaces more than $\sim 55^\circ$ off the equator. We further show on the basis of the sun's path across the sky that penitents that are corrugated, i.e. occur in long ridges or rows, must align their ridge axis within 30° of the east–west transect.

KEYWORDS: energy balance, ice/atmosphere interactions, mountain glaciers, snow/ice surface processes

INTRODUCTION

Penitents are the end expression of instabilities that arise during ablation of snow or ice driven by sunlight where relatively flat surfaces are transformed into large blade-like structures (Fig. 1). In our current climate, penitents typically form on mountain glaciers and snowfields in the tropics and subtropics. The formation of penitents is important because the surface roughness of snowfields is a critical determinant of surface albedo, the remote sensing of snowpack properties (Warren and others,1998; Hudson and others, 2006) and sublimation and melting (Lliboutry, 1999; Corripio and Purves, 2005; Winkler and others, 2009; Cathles and others, 2011). Understanding where and why penitents form, and the physical processes that are most directly responsible for them, are therefore important steps in understanding high-alpine snowpacks.

Despite Darwin's speculation that penitents are carved by wind (Darwin, 1839), it is now widely agreed that the primary driver of penitent formation is sunlight (Odell, 1941; Lliboutry, 1954; Naruse and Leiva, 1997; Betterton, 2001; Bergeron and others, 2006). The basic formation mechanism of penitents, as sketched by Lliboutry (1954), is that geometric focusing of incoming solar radiation causes initial surface undulations to grow. This focusing causes depressions in the surface to receive both direct, incoming insolation and reflected insolation from the surrounding surface. Peaks in the surface only receive direct insolation, and thus do not ablate as quickly as depressions which receive more reflected sunlight. This process leads to the growth of penitent structures. Once initial penitents form, other processes can lead to differential ablation that significantly enhances the growth of penitent features (Lliboutry, 1954; Kotlyakov and Lebedeva, 1974); however, these processes are secondary, because without sunlight, penitents cannot initiate.

Theoretical and experimental work has shown that radiation can drive the formation of surface roughness in snow. Betterton (2001) showed that an ad hoc treatment of geometric focusing of sunlight described by Lliboutry (1954) causes a flat surface to be unstable to ablation from sunlight perpendicular to the surface, and that perturbations spontaneously grow in amplitude. Similar results were found using different mathematical models and confirmed by observations (Tiedje and others, 2006; Mitchell and Tiedje, 2010). Laboratory experiments by Bergeron and others (2006) confirm that small perturbations grow from a horizontal snow surface when illuminated by light directly above the snow surface. These studies did not investigate how the mechanism explains the limited latitudinal extent and east–west orientation of penitents.

Here we extend the work of Betterton (2001) to include large and evolving surface perturbations and varying incidence angles of incoming radiation. The combination of these additions provides insights into the formation mechanism originally put forth by Lliboutry, and shows that his proposed formation mechanism can also be used to explain why penitent formation on flat surfaces is limited to the tropics and subtropics.

GEOGRAPHIC EXTENT AND ORIENTATION OF PENITENTS

Penitents are observed in a restricted latitudinal range and have a consistent orientation. Reported penitent formation is primarily between 37°S (Lliboutry, 1999) and 46°N (Matthes, 1934). First described by Darwin, penitents have since been observed in the Andes (Darwin, 1839; Troll, 1942; Lliboutry, 1954; Hastenrath and Koci, 1981; Lliboutry, 1999; Corripio and Purves, 2005), Asia (Holland, 1910; Odell, 1941; Kotlyakov and Lebedeva, 1974), North America (Matthes, 1934; Nichols, 1939; Amstutz, 1958), Hawaii (Wentworth, 1940) and Africa (Lliboutry, 1954; Kaser and others, 2010), yet penitents are largely absent from polar

*Present address: Department of Atmospheric, Oceanic and Space Sciences, University of Michigan, MI, USA.

https://doi.org/10.3189/2014JoG13J124 Published online by Cambridge University Press

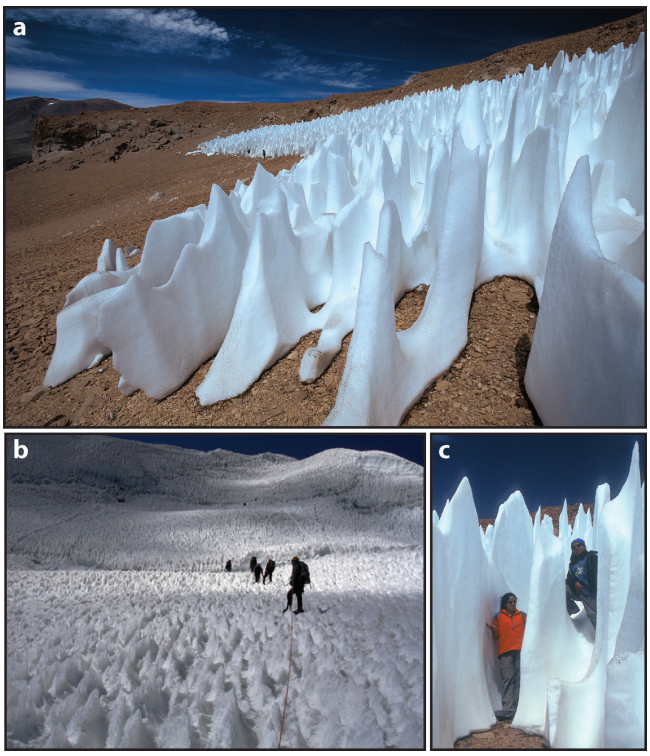

Fig. 1. Three photographs showing important characteristics of penitents: the blade-like characteristics and consistent orientation (a), the prevalence of penitents across large areas and a range of elevations (b), and the range in typical penitent height from 10 cm (b) to 3 m (c). Photographs (a) and (c) were taken by Gerhard Hüdeppohl, and photograph (b) was taken by Douglas Melzer.

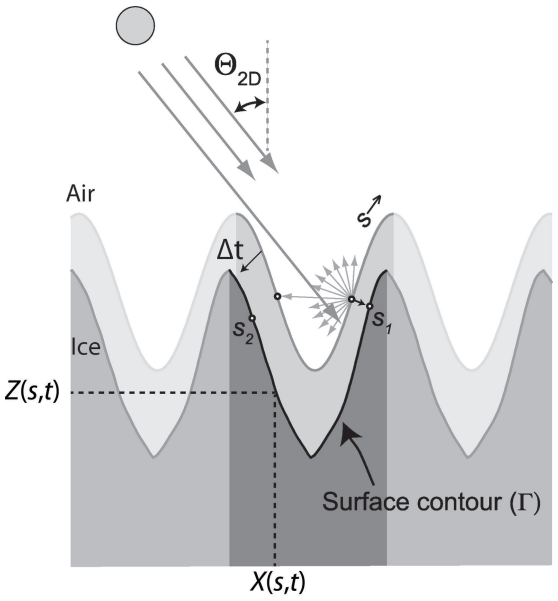

Fig. 2. The domain of the analysis is the curvilinear contour Γ that separates snow or ice (below) from air (above). The domain is periodic, so the analysis is limited to the segment of Γ that is between two crests of the topography. Breaking the domain at crests ensures that no energy can be transmitted between subdomains. The curvature of Γ causes both shadows and indirect radiative exchanges. For example, light incident on point S_1 reflects and adds to the energy absorbed at point S_2, even though S_2 is shadowed by the contour from direct solar illumination. At each time-step δt of the analysis, both the geometry and magnitude of the incoming solar beam are modified to account for the sun's position in the sky, and the surface is modified to account for ablation (denoted by the light-gray shaded region of ice between the initial and final position of the contour).

snow and ice fields such as in Greenland or Antarctica. There are a few reports in the literature describing observations of penitents in Greenland (Odell, 1941) and Antarctica (Wright and Priestley, 1922; Favier and others, 2011), but it is not clear whether these reports reflect structures on surfaces that are significantly out of horizontal or to what extent debris, dust and other factors are at play.

A ubiquitous property of penitents is their consistent orientation (Holland, 1910; Matthes, 1934; Nichols, 1939; Wentworth, 1940; Odell, 1941; Lliboutry, 1954; Kotlyakov and Lebedeva, 1974; Hastenrath and Koci, 1981; Naruse and Leiva, 1997; Corripio and Purves, 2005). The troughs and blades of a field of penitents align east–west, such that the faces point equatorward. Naruse and Leiva (1997) report detailed measurements of penitent orientation, showing that the average ridge orientation of penitents is between –10° and +20° of aligning east–west.

Although it is clear from observations that penitents form predominantly at lower latitudes and with an east–west ridge orientation, these two basic aspects of penitents remain largely unexplained. We use a simplified computational analysis to show that the latitudinal extent and orientation of penitents can be explained by insolation-driven ablation alone. By focusing on a limited set of assumptions, we show that the detailed evolution of the sun's path through the sky determines both the range and orientation of penitent features. Results from our analysis agree with the observations described above, and provide insight into the mechanism determining the geographic range and orientation of penitents.

METHODS

We focus our analysis on intra-surface radiative transfer and the effects of insolation-driven sublimation. We additionally consider the detailed evolution of the sun through the day and year. Our analysis considers a two-dimensional (2-D) snow surface where ablation is determined by diurnally and annually varying insolation received at a particular latitude and orientation. Since penitents are elongated, they are well suited for a 2-D model. In the analysis, we calculate two important quantities: (1) the total energy absorbed as a function of distance along the surface contour and (2) the time evolution of the surface contour. To calculate energy absorption, the time-dependent solar zenith angle and the solar azimuth angle are accounted for. These are used to find the distribution of incident energy on the surface depending on its orientation. The geometry-dependent radiative effects associated with shadowing, multiple reflections and absorption are also treated. To evolve the surface in response to this forcing, we assume that all energy absorbed causes sublimation. Sublimation is assumed to act locally and to ablate the surface of the snow in a direction perpendicular to the surface contour. The domain of our analysis consists of a one-dimensional (1-D) curvilinear contour that represents the snow/air interface. The surface is periodic, such that the first and last node points are the same. Figure 2 depicts the domain and processes included in our analysis. Details of the analysis are described below, and in greater detail by Cathles (2011) and Cathles and others (2011).

https://doi.org/10.3189/2014JoG13J124 Published online by Cambridge University Press

The analysis was performed by computing the evolution of an initial sinusoidal roughness profile in response to a 45 day ablation season. Our analysis determines whether this initial surface grows in amplitude or decays to a flat, horizontal surface. We identify parameters that promote amplitude growth with conditions that favor penitent formation. For all results shown, we used an initial condition where the amplitude of the surface perturbation is the same as the wavelength of the perturbation. This ensures that if the amplitude of the surface roughness grows, the resulting surface roughness will have peaks taller than the distance between them, which is consistent with observations of penitent formations (Corripio and Purves, 2005). The detailed evolution of penitents cannot be explained using our analysis, because we limit our consideration to the physical processes described above, and disregard other aspects of snow and ice energy and mass balance.

Radiative transfer analysis

As shown in Figure 2, we consider a 1-D curvilinear contour Γ that represents the ice/air interface of a transverse cross section of a penitent ridge. Distance along the contour (from left to right) is represented by the curvilinear variable s, and horizontal and vertical Cartesian coordinates are represented by x and z, respectively. The domain is periodic, such that the first point along the contour is the same as the last point, and the domain is always arranged such that the end points are the highest points on the contour. This means that all reflection between points on the surface is contained within a single periodic unit of the penitent field. The contour is discretized into 100 segments. This analysis makes several simplifying assumptions of how incident energy reflects from the surface: there is no angular dependence on the reflectivity of the surface, the ice is assumed to be optically opaque, i.e. all light is absorbed or reflected at the interface, and the albedo is uniform at all wavelengths of incident light.

The central physical element of the analysis is the treatment of shortwave energy within the periodic domain. The absorption of incoming solar energy, E_a, involves the complexity of multiple reflections that is treated following Pfeffer and Bretherton (1987). The energy emitted by reflection at a point s along the surface Γ, $R(s)$, is expressed as a Fredholm integral equation of the second kind:

$$R(s) = R_d(s) + \int_\Gamma \alpha F(s, s') R(s') \, ds' \tag{1}$$

where $R_d(s)$ is the component of direct incoming energy emitted by reflection from s, α is the albedo of the surface material, and $F(s, s')$ is the fraction of energy leaving some other part of the contour at s' which is incident on s. Once $R(s)$ is calculated, the absorbed energy, $E_a(s)$, is relatively straightforward:

$$E_a(s) = E_d(s) + \int_\Gamma (1 - \alpha) F(s, s') R(s') \, ds' \tag{2}$$

where $E_d(s)$ is the energy per unit width absorbed from direct incoming solar radiation. The second term of Eqn (2) integrates all the reflected energy which is incident on point s from all points along the contour. We convert these equations into a system of linear equations for values of the variables at gridpoints along the contour, which we then solve for numerically. Details of these computations have been described elsewhere (Cathles, 2011; Cathles and others, 2011). The important feature of this analysis it that it accounts for all reflections within the periodic domain.

Solar ephemeris in a 2-D plane

A unique feature in our analysis is that we consider the trajectory of the sun through the sky. We follow Walraven (1978) and use spherical trigonometry to determine both the sun's zenith angle (Θ) and azimuth (ϕ). Because penitents are highly linear features, we restrict our consideration to 2-D features, and thus project the sun's three-dimensional (3-D) location into the 2-D plane of our simulation. This can be accomplished by converting the azimuth to an azimuth relative to the projected plane, ϕ_p. The projected zenith angle is then

$$\Theta^p_{2D} = \tan^{-1}\left(\frac{\sin(\Theta)\cos(\phi_p)}{\cos(\Theta)}\right). \tag{3}$$

The insolation must be reduced to account for the energy passing perpendicular to the 2-D plane of the domain. This is accomplished by defining an intensity factor

$$I_p = \sqrt{(\cos(\Theta))^2 + (\sin(\Theta)\cos(\phi_p))^2}. \tag{4}$$

Both the 2-D zenith angle and the intensity factor are derived in Cathles (2011).

The atmosphere is assumed to be cloud-free, and the intensity of incoming insolation perpendicular to the beam of light at ground level is fixed at $1000\,W\,m^{-2}$. This represents a conservatively large attenuation of the top-of-atmosphere flux of $1365\,W\,m^{-2}$ compared to regions where penitents typically form (Corripio and Purves, 2005; Mölg and others, 2009). Observations suggest that 93–95% of incoming light where penitents typically form is direct (Kotlyakov and Lebedeva, 1974; Corripio and Purves, 2005). We thus neglect diffuse light. For simplification, we do not include spectrally dependent reflection and absorption. The start and stop day for each simulation is latitude-dependent, and chosen so that the midpoint of the integration period is the day with maximum solar elevation and our time-step is 15 min. Over the simulation period, the daily average insolation incident on a horizontal surface is a complex function of latitude, but ranges from approximately $320\,W\,m^{-2}$ at the equator to $390\,W\,m^{-2}$ at the poles. The non-monotonic behavior of this function is due to variations in angle of incidence and length of day (Hartmann, 1994, fig. 2.6).

Treatment of ablation

Energy transfer in the ice below the surface is not treated (effectively treating the ice as temperate through the full depth of the ice below the surface), and energy-balance terms associated with sensible and latent heat transfer and longwave radiation are neglected. These assumptions are a critical part of the analysis simplifying the problem so that we can conduct a set of experiments that determine how solar radiation controls penitent formation.

It has been observed that penitents form when the dew point remains below the freezing temperature, which implies, at least initially, sublimation is the ice-removal process (Lliboutry, 1954; Bergeron and others, 2006). The analysis therefore uses sublimation, not melting, as the ablation process. Results for simulations of melting ice where the water is instantaneously removed from the surface do not significantly change our results. It has been suggested that the

https://doi.org/10.3189/2014JoG13J124 Published online by Cambridge University Press

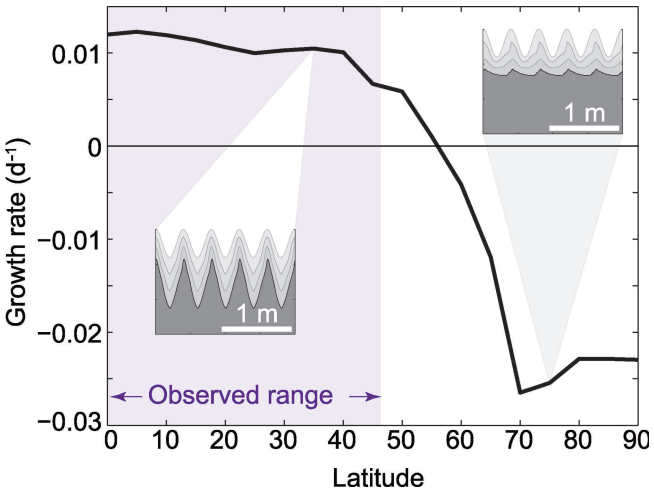

Fig. 3. Penitent growth rate as a function of latitude for east–west-oriented features as calculated over a 45 day ablation season. The growth rate is strongly positive, indicating strong potential for penitent formation, within ~55° of the equator. Insets show evolution of the surface contour, Γ, at 15 day intervals for 35° and 75° poleward of the equator. The change in amplitude of the surface roughness is normalized to the ablation of an equivalent flat surface, so the unit for the growth rate is d^{-1}.

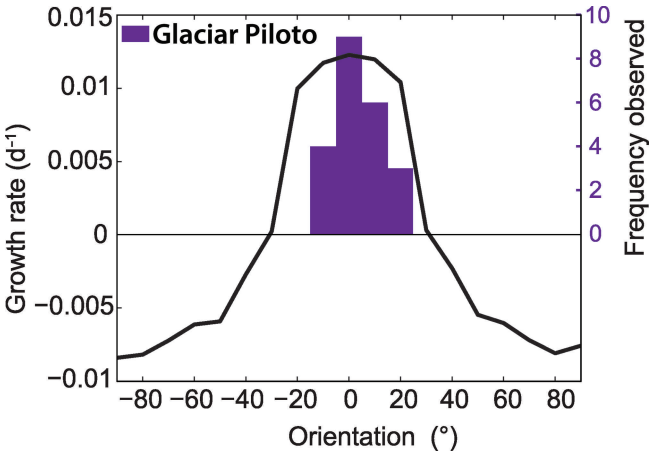

Fig. 4. A comparison of observed penitent orientation frequency and orientations that support penitent formation in our numerical analysis. The bar graph shows reported average orientations for 22 faces of penitents measured on Glaciar Piloto, Argentina (32° S) (Naruse and Leiva, 1997). The line shows the growth rate of the amplitude of the surface topography for the same latitude of Glaciar Piloto, and at the same time as the observations were made (17 December), after 45 days of simulation. For consistency, the same normalization used in Figure 3 is applied to the growth rate calculation shown here.

development of large penitents requires additional processes such as differential ablation (sublimation on the peaks and melting in the trough) (Lliboutry, 1954), a cooling breeze on the peaks (Matthes, 1934), or sediment or ponding of meltwater in the troughs between peaks (Kotlyakov and Lebedeva, 1974). Including these processes would require a detailed microclimate analysis. Our analysis reproduces the observed orientational and latitudinal limits on penitents without including these effects. This indicates that these other effects are of secondary importance.

Given the above assumptions, the ablation rate is calculated at every time-step from the absorbed energy distribution using the following simplification:

$$\dot{H}(s_i) = \frac{E_a(s_i)}{\rho L \cdot \mathrm{d}s_i} \tag{5}$$

where ρ is the density of ice, L is the latent heat of sublimation, and $\mathrm{d}s_i$ is the length of the segment used to discretize Γ. Assuming that the snow or ice ablates in a direction perpendicular to the surface contour, we can convert the ablation rate to a velocity U for any point located on the contour:

$$U = \dot{H}(-\mathbf{n}) \tag{6}$$

where $-\mathbf{n}$ is the into-ice pointing unit vector perpendicular to Γ. The ablation rate is calculated for line segments on the contour Γ, but it is the nodes which must be moved to update the position of Γ. To make this adjustment we adopt the weighted residuals method, the implementation of which is described in detail in Cathles (2011) and Cathles and others (2011). At the end of every time-step we re-mesh using a linear interpolation scheme. This prevents bunching of nodes along the surface, but potentially adds interpolation artifacts such as surface smoothing. We also rearrange the points by shifting the highest node to the first point position in the periodic domain to insure all reflections are contained within one periodic unit.

RESULTS

Depending on latitude, the initial sinusoidal roughness is either enhanced (penitents form) or diminished. Figure 3 shows the growth rate of the amplitude of the surface roughness over a 45 day simulation. Two insets show examples of the surfaces at 35° and 75° off the equator and show the surface at 7 day intervals (the initial surface contour in the lightest gray, and the darkest gray showing the final ablated surface). At low latitudes, the surface evolves into a series of blade-like peaks and valleys, with increasing amplitude as ablation progresses (Fig. 3 inset). At high latitudes, the amplitude of roughness decays as ablation progresses because the sides of a surface feature intercept more high-solar-zenith-angle radiation than the bottom of the depression. The analysis yields strongly positive growth rates at latitudes up to ~40° and weakly positive growth rates up to 55°, which agrees well with the bulk of the observed penitent fields occurring between 37° S and 46° N.

The preferred east–west orientation of penitents also emerges naturally from our calculations (Fig. 4). The orientation angle is the alignment of the peaks and troughs as measured from east to west. As the ridge orientation of the penitent field changes, so does the sun's projection into the perpendicular plane (Fig. 5). For ridge orientations not aligned east–west, the sun's energy is incident over a broader range of angles. This distributes the absorbed energy more evenly on the surface and inhibits the formation of penitents. Figure 4 compares the growth rate of the amplitude of the surface roughness in our simulations over a 45 day period and across the full range of possible orientation angles to a set of observed orientations of penitents from Glaciar Piloto, Argentina (Naruse and Leiva, 1997). Our analysis finds that, at the latitude of Glaciar Piloto (32° S), penitents can only form at an orientation within 30° of the east–west direction. This is consistent with observations from Naruse and Leiva (1997) for the region.

https://doi.org/10.3189/2014JoG13J124 Published online by Cambridge University Press

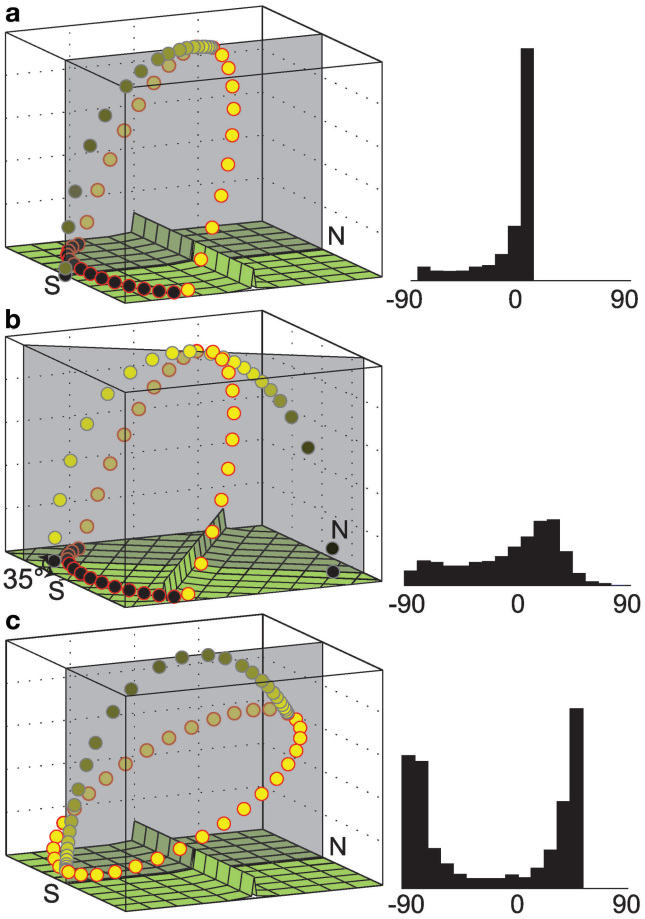

Fig. 5. Sun diagrams (left panels) and associated histograms (right panels) of the elevation angle of incoming solar radiation projected onto the plane (denoted by gray surface) perpendicular to the orientation of surface roughness (denoted by ridge on bottom of panels on the left): (a) east–west-oriented penitent at 32° S; (b) penitent oriented 35° off the east–west orientation at 32° S; and (c) east–west-oriented penitent at 70° S. The yellow disks represent the location of the sun at 45 min intervals on the summer solstice. Disks with gray outline indicate the projection of the sun in the 2-D plane that is perpendicular to the face orientation of the penitent. The darkness of the sun's projected disk indicates the relative intensity of incoming energy incident on the penitent faces.

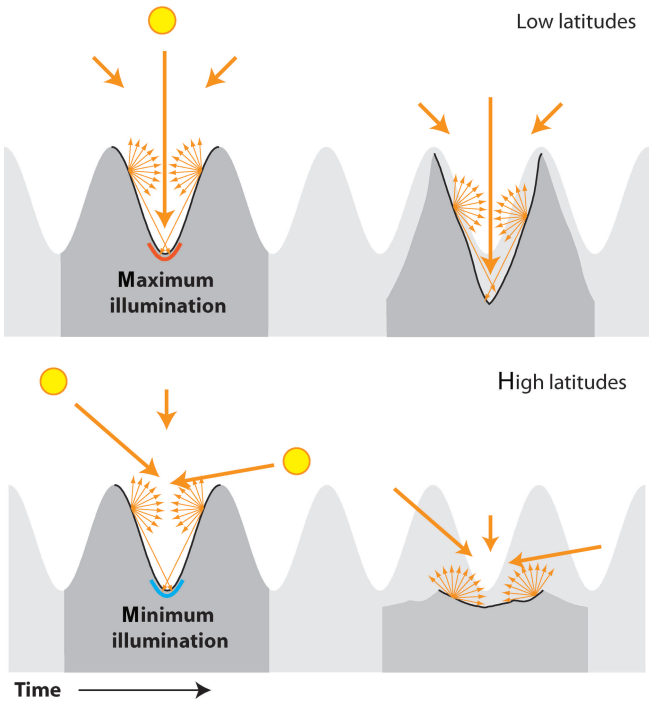

Fig. 6. A schematic summary of the radiative transfer mechanism for penitent formation. The key aspect of this mechanism is that the sun's energy needs to be focused within the 2-D plane of the developing penitent. The bulk of the energy must come from within a narrow range of zenith angles, but the range can be centered on any angle. For horizontal surfaces, this narrow range only occurs within the tropics and subtropics for features oriented east–west (Fig. 4).

DISCUSSION

Surface roughness grows rather than decays when the distribution of incident light is within a narrow range of incident angles. This criterion fails for the polar regions, because there is a bimodal distribution of incident light. Nevertheless, and as an additional proof of the assertion, when the bimodal or widespread distribution of input energy angles is artificially restricted (e.g. by topography, shadowing, non-horizontality, diurnal variations in clouds, etc.), surface roughness features will grow in polar regions too. The fact that penitents are rare in polar regions is an affirmation of the basic theory that penitents require the variation in the angles of incoming solar radiation to be small.

The latitudinal and orientational limitations on penitent formation shown in Figures 3 and 4 result from the same mechanism: the distribution of incident angles of incoming radiation (Fig. 6). At low latitudes, for features with an east–west orientation, incoming energy is primarily incident within a narrow range of angles (Fig. 5a). As shown in Figure 5b, when features are not aligned east–west, the insolation is evenly distributed. While an even distribution does generate geometric focusing of radiation towards the base of a surface perturbation, this effect is not strong enough to counter the ablation along the sides of surface perturbations. Initial surface roughness at low latitudes, when not aligned east–west, will thus decay. At high latitudes, the angles of incoming energy are distributed bimodally (Fig. 5c). This also causes ablation on both sides of initial surface perturbations and induces them to decay. If part of the bimodal illumination from the sun were blocked from the surface, either by the slope of the surface itself, or by the shadow of mountains, penitents could be induced to form at high latitudes, because the remaining portion of insolation would be concentrated into a narrower band of angles of incidence. Penitents could also possibly form with orientations that depart from east–west if the surface were shadowed for parts of a day. While our analysis was not intended as a comprehensive model of penitent structures, the computations we show here do a reasonable job of simulating observed surfaces. Figures 7 and 8 compare sketches of penitents found in the literature with model results. Figure 8 compares a computed result with detailed observations at Glaciar Piloto (32.6° S). Naruse and Leiva (1997) describe the average of 11 penitents: 'The surface slope on the southern face ranged from about 60 to 85°. It is clearly recognized that the slope of the northern face is steeper with a negative angle (overhung) and almost coincides with the solar angle at noon on the summer solstice.' These observations were made 2 days before the summer solstice. The results of our analysis when applied to

https://doi.org/10.3189/2014JoG13J124 Published online by Cambridge University Press

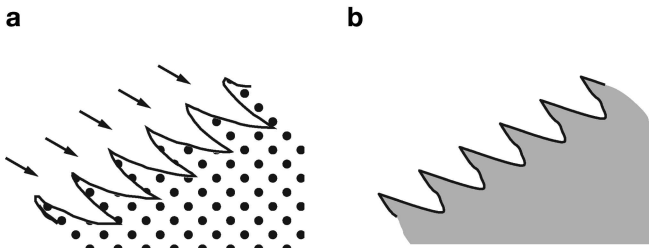

Fig. 7. Penitents have been on occasion reported in both Antarctica and Greenland. The only report with details describes penitents found in Antarctica on Koettlitz Glacier at 78° S (Wright and Priestley, 1922). The surface was north-facing and steeply sloped at 30°. A trace of a sketch shown in figure 98 in Wright and Priestley (1922) (a) is compared with simulated penitents (b). Simulations were run for 45 days leading up to the summer solstice. As a result of the steep surface slope, the radiative transfer mechanism produces penitents that roughly agree with observations.

the same latitude after 90 days of simulation leading up to the summer solstice compare well with these observations. We find a very slight overhang on the north side, and the slope of the southern face is 57°.

Sensitivity

The initial surface contour used as the starting point of our computation experiments has a horizontal wavelength that is the same as the peak-to-trough amplitude. This ensures that any growth in amplitude brings the surface into a regime where the peaks are taller than the distance separating them, an observation often made regarding penitent features (Lliboutry, 1999; Corripio and Purves, 2005). Experiments with a higher aspect ratio (width:height) expand both the latitudinal range and the domain orientation where our analysis shows amplitude growth (for further details, see Cathles, 2011, fig. 6.9). This does not contradict observations, as suncup features (Rhodes and others, 1987; Betterton, 2001; Mitchell and Tiedje, 2010) are found at higher latitudes and do not exhibit directionality. Suncups are short, 3-D perturbations to the surface where the width of the feature is greater than the depth of the perturbation. Since suncups are not 2-D features, our model is not well suited to further explore their formation.

It has also been suggested that penitents cannot form in snowfields with high surface albedos (Kotlyakov and Lebedeva, 1974). We did not investigate the initial formation of surface roughness; however, once initial roughness is present, we do not find that higher albedo reduces the propensity to form penitents. When the surface albedo is increased from 0.6 to 0.8 the overall ablation decreases, but we find that the normalized growth rate of penitents actually increases. In general, our results are robust to changes in the physical properties of snow. For example, the trends shown in Figures 3 and 4 do not change for surface albedo different from our standard value of 0.6.

Geographic exceptions

Penitents have been reported at high latitudes (Wright and Priestley, 1922; Odell, 1941; Favier and others, 2011). The most detailed report of high-latitude penitents comes from observations on Koettlitz Glacier, Antarctica, where they formed on a steep (30°) north-facing slope (Wright and Priestley, 1922). Figure 7 compares a sketch of penitents (although Wright and Priestley (1922) refer to these features

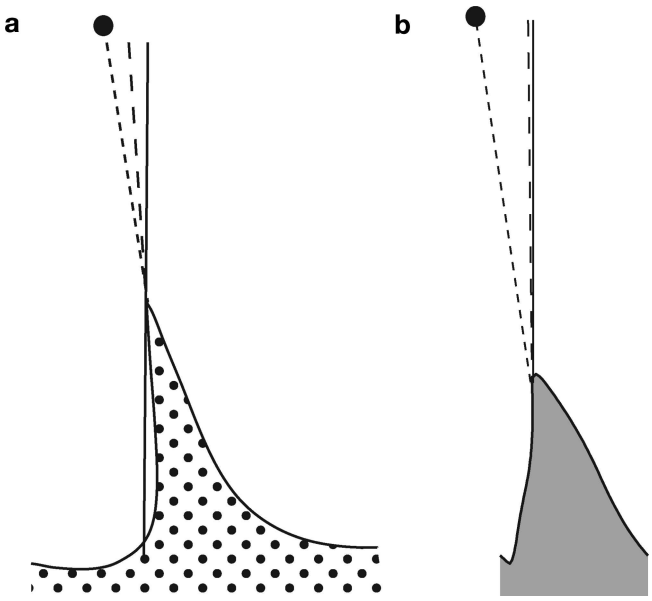

Fig. 8. Detailed comparison of the shape of observed penitents (a) and the geometry computed by the radiative transfer analysis of penitents (b) after 90 days of simulation. The sketch of observed penitents represents an average of 11 cross sections at Glaciar Piloto traced from figure 9 of Naruse and Leiva (1997). The black circle represents the location of the noon sun, with a short-dashed line connecting the peak to the sun. The solid lines show the vertical, and the long-dashed line extends the slope of the north face. The computed penitents are oriented towards the noon sun, and there is a slight overhang present. The base of the modeled penitent is thicker than is observed. This is likely a result of uniform ablation used in the model; if absorbed energy at the base were used to melt, not sublimate as is used at the top of the penitent, significantly more melting would occur, increasing both the depth and the width of the trough.

as 'ploughshares') observed during the British Antarctic expedition of 1910–13 on the north-facing slope of Koettlitz Glacier at 78° S. Our analysis is able to recreate these features because the steep surface slope acts to modify the bimodal insolation distribution characteristics of high latitudes.

There are many unique situations that could limit the daily incident solar energy to a narrow range of zenith angles outside the range needed for penitent growth. The simulations for Koettlitz Glacier provide one such example. Persistent clouds at a particular time each day or shadowing from mountains could also produce penitent growth at high latitudes. The bulk of incident energy at the high latitudes arrives from low-elevation angles, so even distant mountains or slight slopes could affect the distribution of incident insolation. The results here do not prohibit the formation of penitents at high latitudes but they do suggest that special circumstances in surface geometry, shadowing and cloudiness are needed at high latitudes to produce penitents. This may explain why penitent fields are relatively rare in Antarctica and Greenland.

Surface-roughness albedo

Perhaps the most significant result of the analysis presented here is that surface roughness reduces the effective albedo of a snow surface. This means that the energy balance of a snow surface is influenced not only by the microscopic properties of the material forming the surface (e.g. the properties of snow), but also by the macroscopic properties

https://doi.org/10.3189/2014JoG13J124 Published online by Cambridge University Press

of the surface, i.e. how rough it is and whether there is geometry that traps radiation. Figure 9 shows the average daily effective albedo (the ratio of energy reflected back to the atmosphere by the rough surface to the total energy incident on the rough surface; see Cathles and others (2011) for further discussion of effective albedo) for surfaces covered with penitents with three different snow albedos. The effective albedo was calculated over one periodic unit (peak to peak), ensuring that all insolation entering the unit was either absorbed within the region or reflected back to the atmosphere. In each case, the effective albedo is significantly less than the albedo of the surface material. For a snow albedo of 0.6, the effective albedo of a penitent field is reduced to 0.33 simply by the effect of radiation trapping within the roughness. The increase of absorbed energy relative to a flat surface is a factor of 1.67. Our analysis of how surface albedo is influenced by roughness is consistent with published observations (Lliboutry, 1999; Corripio and Purves, 2005) and with Monte Carlo modeling of sunlight-trapping by sastrugi (Warren and others, 1998, fig. 13). However, one previous study of the energy balance of penitent-covered surfaces suggested that there was a reduction in absorbed shortwave radiation (Corripio and Purves, 2005). We think that result is in error, and suggest that both the proper treatment of the geometric focusing effect of surface roughness with the integral-equation-based method used here and careful consideration of the effective albedo are necessary for an accurate account of penitent energy balance. We therefore suggest that penitent formation can accelerate mountain-glacier loss and speed seasonal snowpack runoff. This is an important factor to consider when planning water management (Corripio and Purves, 2005; Vuille and others, 2008). Additionally, penitent formation may have been important in past climates in which large ice sheets existed equatorward of 55°. For example, penitent formation may have affected the southern margins of the Laurentide ice sheet, which reached latitudes lower than 42° N. Radiative trapping by surface roughness could also have reduced the tropical albedo during Neoproterozoic global glaciations, which is crucial for the termination of these events (Abbot and Pierrehumbert, 2010). A recent study suggests penitents may not be restricted to Earth and may play a role in the energy balance of icy planets (Hobley and others, 2013). The latitudinal range of penitents would depend on the planet's orbital parameters.

CONCLUSIONS

Penitents have remained mysterious snow-surface features since they were documented by Charles Darwin. We have shown using radiative transfer analysis featuring surface-to-surface shortwave energy exchange, and driven only by sunlight, that the observed orientational and latitudinal limits on penitent formation result directly from the detailed evolution of the sun through the sky. The critical factor determining whether penitents can form is the degree to which daily incoming energy is focused within a narrow range of incident angles. For horizontal surfaces, this criterion is only met at low latitudes for east–west-oriented ridges. While the radiative transfer analysis presented here was not designed to encompass all the physical processes involved in the formation of penitents, it captures the essential irreducible mechanism for penitent formation.

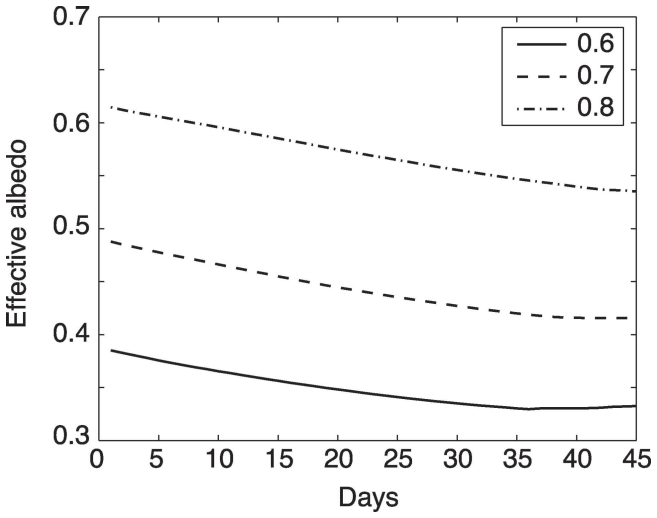

Fig. 9. Evolution of the effective surface albedo for three snow albedos for simulations run for 45 days starting on 6 November at 32° S and for penitents oriented east–west. The reduction in surface albedo is significant and robust. Absorbed energy is up to 1.67 times higher than for a flat horizontal surface with the same snow albedo (0.6).

More general models of snow and ice surfaces do not permit the spontaneous formation of penitent fields because they lack the integral-equation formulation of surface-to-surface radiative transfer essential to the growth of penitents. We further find that the penitent-like surfaces created by the analysis shown here have significantly lower effective albedos than a smooth horizontal surface. Thus the presence of penitent fields may increase the rate of snowmelt.

ACKNOWLEDGEMENTS

This research was supported by US National Science Foundation (NSF) grant ARC-0907834. We thank Stephen Warren and Javier Corripio for comprehensive and constructive comments on early drafts of this paper, and two reviewers and the Scientific Editor Tomas Mölg for substantially improving the manuscript. We also thank Gerhard Hüdeppohl and Douglas Melzer for the use of their photographs.

REFERENCES

Abbot DS and Pierrehumbert RT (2010) Mudball: surface dust and snowball Earth deglaciation. *J. Geophys. Res.*, **115**(D3), D03104 (doi: 10.1029/2009JD012007)

Amstutz GC (1958) On the formation of snow *penitentes*. *J. Glaciol.*, **3**(24), 304–311

Bergeron V, Berger C and Betterton MD (2006) Controlled irradiative formation of penitentes. *Phys. Rev. Lett.*, **96**(9), 098502 (doi: 10.1103/PhysRevLett.96.098502)

Betterton MD (2001) Theory of structure formation in snowfields motivated by penitentes, suncups, and dirt cones. *Phys. Rev. E*, **63**(5), 56129

Cathles LM (2011) *Radiative energy transport on the surface of an ice sheet.* (PhD thesis, University of Chigago)

Cathles LM, Abbot DS, Bassis JN and MacAyeal DR (2011) Modeling surface-roughness/solar-ablation feedback: application to small-scale surface channels and crevasses of the Greenland ice sheet. *Ann. Glaciol.*, **52**(59), 99–108 (doi: 10.3189/172756411799096268)

https://doi.org/10.3189/2014JoG13J124 Published online by Cambridge University Press

Corripio J and Purves R (2005) Surface energy balance of high altitude glaciers in the central Andes: the effect of snow penitents. In De Jong C, Collins DN and Ranzi R eds. *Climate and hydrology of mountain areas*. Wiley, Chichester, 15–27

Darwin C (1839) *Voyage of the Beagle*. P.F. Collier and Son Corporation, New York

Favier V, Agosta C, Genthon C, Arnaud L, Trouvillez A and Gallée H (2011) Modeling the mass and surface heat budgets in a coastal blue ice area of Adelie Land, Antarctica. *J. Geophys. Res.*, **116**(F3), F03017 (doi: 10.1029/2010JF001939)

Hartmann DL (1994) *Global physical climatology*. Academic Press, San Diego, CA

Hastenrath S and Koci B (1981) Micro-morphology of the snow surface at the Quelccaya ice cap, Peru. *J. Glaciol.*, **27**(97), 423–428

Hobley DEJ, Moore JM and Howard AD (2013) How rough is the surface of Europa at Lander scale? [Abstr. 2432] In *44th Lunar and Planetary Science Conference, 18–22 March 2013, The Woodlands, Texas, USA*. http://www.lpi.usra.edu/meetings/lpsc2013/pdf/2432.pdf

Holland TH (1910) Mountaineering in the North-West Himalaya. *Nature*, **84**(2125), 78–80 (doi: 10.1038/084078a0)

Hudson SR, Warren SG, Brandt RE, Grenfell TC and Six D (2006) Spectral bidirectional reflectance of Antarctic snow: measurements and parameterization. *J. Geophys. Res.*, **111**(D18), D18106 (doi: 10.1029/2006JD007290)

Kaser G, Mölg T, Cullen NJ, Hardy DR and Winkler M (2010) Is the decline of ice on Kilimanjaro unprecedented in the Holocene? *Holocene*, **20**(7), 1079–1091 (doi: 10.1177/0959683610369498)

Kotlyakov VM and Lebedeva IM (1974) Nieve and ice penitentes: their way of formation and indicative significance. *Z. Gletscherkd. Glazialgeol.*, **10**(1–2), 111–127

Lliboutry L (1954) The origin of penitents. *J. Glaciol.*, **2**(15), 331–338

Lliboutry L (1999) Glaciers of the dry Andes. In Williams RS Jr and Ferrigno JG eds. *Satellite image atlas of glaciers of the world: South America*. (USGS Professional Paper 1386-I) US Geological Survey, Reston, VA, I119–I147

Matthes FE (1934) Ablation of snow-fields at high altitudes by radiant solar heat. *AGU Trans.*, **15**(2), 380–385 (doi: 10.1029/TR015i002p00380)

Mitchell KA and Tiedje T (2010) Growth and fluctuations of suncups on alpine snowpacks. *J. Geophys. Res.*, **115**(F4), F04039 (doi: 10.1029/2010JF001724)

Mölg T, Cullen NJ and Kaser G (2009) Solar radiation, cloudiness and longwave radiation over low-latitude glaciers: implications for mass-balance modelling. *J. Glaciol.*, **55**(190), 292–302 (doi: 10.3189/002214309788608822)

Naruse R and Leiva JC (1997) Preliminary study on the shape of snow penitents at Piloto glacier, the central Andes. *Bull. Glacier Res.*, **15**, 99–104

Nichols RL (1939) Nieves penitentes near Boston, Massachusetts. *Science*, **89**(2320), 557–558 (doi: 10.1126/science.89.2320.557)

Odell NE (1941) Ablation at high altitudes and under high solar incidence. *Am. J. Sci.*, **239**(5), 379–382 (doi: 10.2475/ajs.239.5.379)

Pfeffer WT and Bretherton CS (1987) The effect of crevasses on the solar heating of a glacier surface. *IAHS Publ.* 170 (Symposium at Vancouver 1987 – *The Physical Basis of Ice Sheet Modelling*), 191–205

Rhodes JJ, Armstrong RL and Warren SG (1987) Mode of formation of 'ablation hollows' controlled by dirt content of snow. *J. Glaciol.*, **33**(114), 135–139

Tiedje T, Mitchell KA, Lau B, Ballestad A and Nodwell E (2006) Radiation transport model for ablation hollows on snowfields. *J. Geophys. Res.*, **111**(F2), F02015 (doi: 10.1029/2005JF000395)

Troll C (1942) Büsserschnee (Nieve de los penitentes) in den Hochgebirgen der Erde: ein Beitrag zur Geographie der Schneedecke und ihrer Ablationsformen. *Petermanns Geogr. Mitt.* 240

Vuille M and 6 others (2008) Climate change and tropical Andean glaciers: past, present and future. *Earth-Sci. Rev.*, **89**(3–4), 79–96 (doi: 10.1016/j.earscirev.2008.04.002)

Walraven R (1978) Calculating the position of the Sun. *Sol. Energy*, **20**(5), 393–397 (doi: 10.1016/0038-092X(78)90155-X)

Warren SG, Brandt RE and Hinton OP (1998) Effect of surface roughness on bidirectional reflectance of Antarctic snow. *J. Geophys. Res.*, **103**(E11), 25 789–25 805 (doi: 10.1029/98JE01898)

Wentworth CK (1940) Ablation of snow under the vertical sun in Hawaii. *Am. J. Sci.*, **238**(2), 112–116 (doi: 10.2475/ajs.238.2.112)

Winkler M, Juen I, Mölg T, Wagnon P, Gómez J and Kaser G (2009) Measured and modelled sublimation on the tropical Glaciar Artesonraju, Perú. *Cryosphere*, **3**(1), 21–30 (doi: 10.5194/tc-3-21-2009)

Wright CS and Priestley RE (1922) *British (Terra Nova) Antarctic Expedition 1910–13. Glaciology*. Harrison, London

MS received 14 June 2013 and accepted in revised form 12 October 2013